Spatial correlation between Bi atoms in dilute $GaAs_{1-x}Bi_x$: From random distribution to Bi pairing and clustering

G. Ciatto,[1,*] E. C. Young,[2] F. Glas,[3] J. Chen,[4] R. Alonso Mori,[4] and T. Tiedje[2]
[1]*Synchrotron SOLEIL, L'Orme des Merisiers, Saint-Aubin, BP 48, 91192 Gif-sur-Yvette Cedex, France*
[2]*Department of Physics and Astronomy, University of British Columbia, Vancouver, British Columbia, Canada V6T 1Z1*
[3]*Laboratoire de Photonique et de Nanostructures, CNRS, Route de Nozay, 91460 Marcoussis, France*
[4]*European Synchrotron Radiation Facility, BP 220, 38043 Grenoble Cedex 9, France*
(Received 4 June 2008; published 23 July 2008)

We use x-ray absorption spectroscopy to investigate the local structure around Bi atoms in $GaAs_{1-x}Bi_x$ layers grown on GaAs as a function of Bi concentration in order to detect short-range order. We find that static disorder in the Bi next-nearest-neighbor interatomic distances dramatically increases when the Bi concentration is increased. At 1.2% Bi concentration, the Bi atoms are randomly distributed whereas at 1.9%, they tend to form next-nearest-neighbor pairs. When the Bi concentration rises to 2.4%, our results suggest that some of the Bi atoms form small Bi clusters. Such strong deviations from a random distribution are likely to play an important role in the occurrence of the giant optical bowing recently measured in this alloy.

DOI: 10.1103/PhysRevB.78.035325 PACS number(s): 81.05.Ea, 61.05.cj, 42.55.Px, 61.66.Dk

I. INTRODUCTION

Long-wavelength infrared devices on GaAs substrates offer important advantages over competing approaches, such as growth on InP substrates. In order to obtain GaAs-based 1.3–1.55 μm emitters and 1 eV band-gap components for multijunction solar cells,[1] GaAs alloys with N,[2] In,[3] and Sb (Ref. 4) have recently attracted much attention. In particular, in dilute nitride semiconductors,[5] the conduction-band minimum is pushed downward due to the perturbation of the host conduction-band-edge states caused by the incorporation of the light N atoms: this induces an anomalously large optical bowing which gives access to the useful wavelength range.[6] However, the use of dilute nitrides in devices presents some intrinsic drawbacks: in particular, the electron mobility is strongly inhibited[7] and the short carrier diffusion lengths limit their integration in solar cells.[1]

Recently, important progress has been made in incorporating Bi into GaAs. $GaAs_{1-x}Bi_x$ alloys containing up to 3% Bi, with good structural quality and strong photoluminescence (PL) emission without need of annealing, have been grown by molecular-beam epitaxy.[8] The interest in *dilute bismides* alloys is threefold: First, since Bi incorporation perturbs the valence-band maximum instead of the conduction-band minimum,[9] this does not affect the electron mobility.[7] Second, for the same alloy concentration, Bi redshifts the band gap by more than four times as much as Sb or In (Ref. 10): this would enable a GaAs-lattice matched $GaAs_{1-x-y}Bi_xN_y$ alloy emitting at 1.55 μm with smaller N concentration (N=2% and Bi=3.5%) and therefore with less deterioration of the transport properties. Finally, in $GaAs_{1-x}Bi_x$, an anomalously large spin-orbit splitting has recently been detected[11] and tailoring spin-orbit interaction by isoelectronic doping opens exciting possibilities in the field of spintronics. Several questions about the properties of the $GaAs_{1-x}Bi_x$ alloy remain open: for example, the origin of the observed giant reduction in the band gap upon Bi incorporation is still controversial since *ab initio* density-functional theory calculations predict an almost "regular" bowing parameter of −2.1 eV,[12] while recent self-consistent pseudopotential-based charge patching methods better reproduce the larger bowing parameter (−5.6 eV) observed in experiments.[9] The efficient PL emission is also surprising, considering the low growth temperature which is normally associated with excess As incorporation and poor electronic properties.[13]

In the present work, we address some of these open issues by investigating the atomic neighborhood and the local distortions around Bi atoms in $GaAs_{1-x}Bi_x$ via extended x-ray absorption fine-structure spectroscopy (EXAFS) and interpreting the experimental data via valence force field (VFF) calculations. It is well known that short-range ordering affects the optical properties of dilute nitrides: for example, In-N preferential binding blueshifts the band gap of $In_xGa_{1-x}As_{1-y}N_y$,[14–16] and like-atoms association in one of the two zinc-blende sublattices (clustering) induces a redshift of the band gap as in the case of N-N correlations in $GaAs_{1-x}N_x$ and In-In in $In_xGa_{1-x}N$.[17] Here, we give evidence that Bi impurities tend to correlate in $GaAs_{1-x}Bi_x$. Determining whether there are Bi next-nearest-neighbor clusters present and their density is important since, similar to N, Bi clusters are likely to induce shallow bound states in the band gap.

II. SAMPLES AND EXPERIMENTAL METHODS

We investigated three $GaAs_{1-x}Bi_x$ samples grown by molecular-beam epitaxy on GaAs substrates with Bi concentrations ranging from 1.2% to 2.4%. Details of the growth procedure and concentration measurements are given in Ref. 8; the samples characteristics are reported in Table I. The change in the band gap with Bi concentration, as determined from the room-temperature PL peak position (column IV), is in agreement with the large redshift previously measured.[8,10] X-ray-diffraction rocking curves attest to the absence of both plastic relaxation and phase separation at large scale: the samples are under pseudomorphic deformation, as we can

TABLE I. Samples characteristics: Bi concentration, thickness, PL peak position, and PL peak full width at half maximum (FWHM).

Sample	Bi (%)	Thickness (nm)	PL peak (nm)	PL FWHM (nm)
A	1.2	270 ± 15	958	36
B	1.9	210 ± 10	984	58
C	2.4	210 ± 10	1014	91

infer from x-ray-diffraction peaks with in-plane components that match the substrate (not shown).

Performing an EXAFS experiment at the Bi L edge on thin $GaAs_{1-x}Bi_x/GaAs$ epilayers is extremely challenging due to the weakness of the signal and to the closeness of the Bi L- and (Ga, As) K-fluorescence lines. Moreover, detecting deviations from random statistics in the distribution of Bi atoms requires the measurement of reproducible EXAFS oscillations with good statistics up to high values of the photoelectron wave number k: in fact the Bi backscattering amplitude is severely damped with respect to the As one in the region $5 \leq k \leq 8$ Å^{-1} so that higher k values are precious in order to recover Bi sensitivity. To this end, an x-ray probe of not only high intensity (flux of 4×10^{10} photons/s at 16 keV) but also exceptional collimation and stability (reproducibility and resolution in energy scans better than $\Delta E/E = 5 \times 10^{-5}$, stabilization of the power incident on the monochromator optical surfaces, and noise to signal in the beam intensity monitor lower than 8×10^{-3}) is mandatory: these requirements are met by the BM29 beamline of the European Synchrotron Radiation Facility (ESRF),[18] where the experiment was performed with a Si-111 monochromator in fluorescence detection mode[19] with a 13-element Ge detector. We selected the Bi $L\beta 1$ emission line (Bi $L\alpha 1$ is too close to the substrate K lines) and recorded EXAFS spectra at the Bi $L2$ edge. In order to reduce thermal damping and, at the same time, to extract a signal free of distortions originating from possible excitation of a stationary wave field in the sample,[20] the epilayers were mounted on a sample holder developed at BM29.[21] The holder permits the sample to rotate and be cooled simultaneously, maintaining a stable temperature (90 K) and eliminating all distortions.

III. RESULTS AND DISCUSSION

Despite the experimental difficulties, high-quality Bi $L2$-edge EXAFS spectra have been obtained on all samples up to $k = 12.5$ Å^{-1}; EXAFS $k\chi(k)$ spectra, extracted from the raw data with the ATHENA code,[22] are shown in the inset of Fig. 1: at first sight, they differ only in the k region of 8.5–12.5 Å^{-1} where the signal from second shell Bi atoms recovers from the amplitude loss present at lower k. $\chi(k)$ data were k^2 weighted and Fourier transformed in the k range (3.2–12.4 Å^{-1}). Figure 1 shows the Fourier transform (FT) for the three samples. Comparing the FT of samples A and B, the first evident difference is that, despite an almost identical amplitude of the first and third main peaks, the second peak

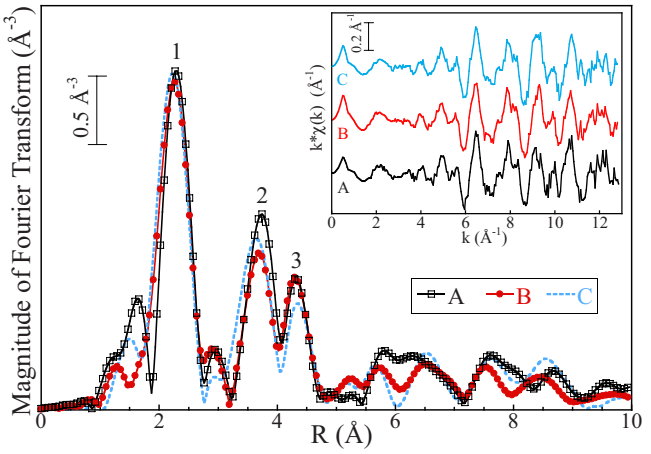

FIG. 1. (Color online) Fourier transform of the Bi $L2$-edge EXAFS signal for the three samples. The three main peaks are labeled. Inset: background subtracted $k*\chi(k)$ spectra.

is strongly damped in sample B. The three main peaks correspond to the different atomic coordination shells around Bi so that the damping affects the mixed Bi-As shell. In standard EXAFS analysis on crystalline materials, theoretical signals are often generated starting from atomic positions given by x-ray diffraction. Some of the interatomic distances are possibly allowed to vary freely and thermal and structural disorders are accounted for by a Debye-Waller parameter for each shell. This was also the approach followed by Ofuchi *et al.*[23] in analyzing $InAs_{1-x}Bi_x$ samples; the authors observed a damping in the amplitude of all atomic shells with increasing Bi concentration, which was attributed to increasing structural disorder. In our case the situation is different because we observe a decrease in amplitude of the sole second shell peak, suggesting an origin associated with a different distribution of Bi and As atoms in the second shell around Bi (thermal disorder is identical since all samples were measured at the same temperature). To analyze these data, we used a strategy that we recently devised and applied to $GaAs_{1-x-y}Sb_xN_y$,[24] aimed at taking precisely into account structural disorder and associated EXAFS signal damping in the case of mixed atomic shells. The method is based on the calculation of the EXAFS theoretical signals using the FEFF 8.1 code[25] performed on simulated crystals. In the simulated crystals atoms occupy sites either randomly or to realize a particular type and degree of short-range order; the static displacement of these atoms from the average crystal sites is determined by VFF calculations. In the present case, the EXAFS simulations were carried out on Bi-centered samples of 381 atoms, containing 4 Bi and 197 As atoms. Nonrandom samples were obtained by placing other Bi atoms around the central Bi to realize the particular short-range order of interest. In order to establish the boundary conditions necessary for the VFF minimization procedure, these samples were embedded into much larger cubic zinc-blende $GaAs_{1-x}Bi_x$ crystals (consisting of 216 000 atoms, i.e., 30 cubic unit cells in each direction) with an average Bi concentration of 1.9%. In the embedding part of the crystal, the Bi atoms were placed at random. The equilibrium atomic positions of all the atoms in the large crystals were found by minimizing the VFF en-

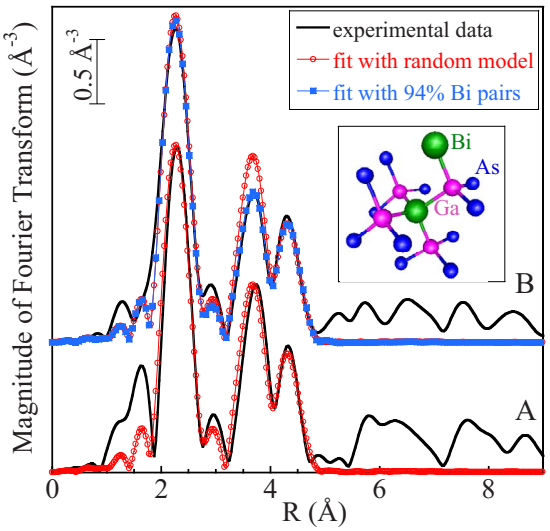

FIG. 2. (Color online) Experimental and simulated Fourier-transformed EXAFS spectra for samples A (bottom) and B (top). The fits are based on clusters with either a random distribution of Bi atoms [red (light gray), open circles] or a predominance of Bi pairs [blue (dark gray), filled squares, see sketch in the inset].

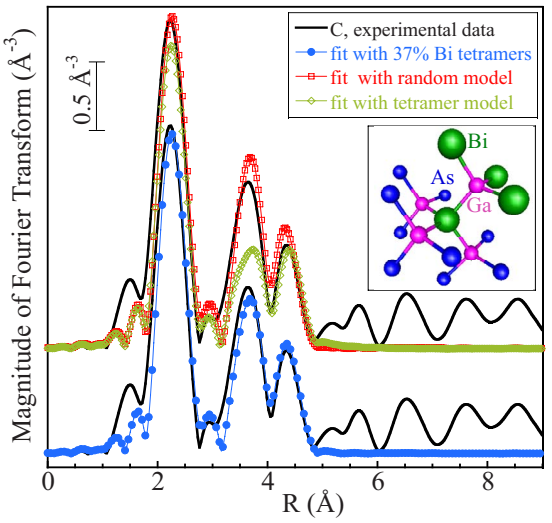

FIG. 3. (Color online) Experimental Fourier-transformed EXAFS spectrum for sample C (continuous black line, top and bottom) and fits performed for clusters with a random anions distribution [red (light gray), open squares], a Bi tetramer [olive (light gray), open diamonds, see sketch in the inset], and a combination of different local configurations as detailed in the text [blue (dark gray), filled circles].

ergy, as detailed previously[26] using calculated values of the lattice parameter and elastic constants for the binary compound GaBi.[27] Theoretical EXAFS signals were then Fourier transformed together with the experimental ones, and fits were performed in the 1.3–4.8 Å R range using the ARTEMIS code.[22]

The spectrum from sample A is well fitted with a random distribution of anions (Fig. 2, bottom). All the EXAFS paths generated from the VFF cluster (the degeneracy of crystallographic data is removed due to the disorder) were used in the fit and interatomic distances were fixed to the calculated values using a unique Debye-Waller variable for each shell. We have used a Gaussian-type Debye-Waller broadening. The values of the structural parameters extracted from the fit are reported in Table II. Note that if Bi is randomly distributed, we are not sensitive to its contribution in the second shell because of the low Bi content. (The probability of a next-nearest-neighbor dimer is 13%.)

As for sample B (Fig. 2, top), if we fix the Debye-Waller values to those determined for sample A, it is evident that the second shell peak cannot be reproduced by a random model [red (light gray), open circles]. Increasing the second shell Bi-As Debye-Waller factor by 25% (i.e., significantly over the 1σ error bar reported in Table II for sample A) provides an apparently satisfactory fit; however, our aim is to go beyond this purely phenomenological procedure and to identify the actual configuration responsible for the signal damping, rather than fitting the data by artificially modifying the Debye-Waller factor to incorporate indiscriminately the effects of static and thermal displacements. We found that the experimental data for samples B and C can be fitted by considering a combination of only three different local configurations: a next-nearest-neighbor Bi pair (inset of Fig. 2), a Bi tetramer (inset of Fig. 3), and a random Bi distribution. In the tetramer configuration, the central Bi atom is surrounded by three Bi next-nearest-neighbors, in a way that all Bi atoms are next nearest neighbors of each other. The procedure consists of simulating the EXAFS spectra by a weighted sum of simulated spectra for each configuration (which depend both on the particular atomic distribution around the central Bi and on the atomic displacements) and using the relative weights as free variables in the fit. In order to keep the number of free parameters to an absolute minimum, for each model we fixed the interatomic distances to the values calculated by VFF and the Debye-Waller factors to the values extracted for sample A. In the case of sample B, we get an excellent best fit [top, blue (dark gray), filled squares] with

TABLE II. Structural parameters extracted from fits to the EXAFS data. Calculated interatomic distances are given as average values. $R_{\text{Bi-}X}$ is the distance between the central Bi atom and its X neighbor and $\sigma^{y\text{th shell}}_{\text{Bi-}X}$ is the Bi-X Debye-Waller factor in the yth atomic shell.

Sample	Bi pairs (%)	Bi tetramers (%)	Random (%)	$R_{\text{Bi-Ga}}$ (Å)	$R_{\text{Bi-As}}$ (Å)	$R_{\text{Bi-Bi}}$ (Å)	$\sigma^{\text{first shell}}_{\text{Bi-Ga}}$ (10^{-3}Å^2)	$\sigma^{\text{second shell}}_{\text{Bi-As}}$ (10^{-3} Å^2)
A			100	2.627	4.048		2.27 ± 0.41	5.2 ± 0.7
B	94 ± 17	6 ± 17	0 ± 24	2.621	4.058	4.097	2.27 (fixed)	5.2 (fixed)
C	0 ± 4	37 ± 19	63 ± 19	2.619	4.049	4.193	2.27 (fixed)	5.2 (fixed)

$94 \pm 17\%$ Bi pairs and $6 \pm 17\%$ Bi tetramers (0% random configuration). However, if we fix the Bi pairs percentage to 100%, the agreement between our simulation and experiment does not significantly worsen; moreover we obtain very similar results when combining random, pairs, and other short-range order configurations such as Bi triplets or different Bi tetramers where Bi next nearest neighbors are linked to different Ga atoms. This result strongly supports the hypothesis that Bi pairs form when the Bi concentration increases from 1.2% to 1.9%. Due to measurement uncertainties, we cannot rule out the possibility that other configurations exist, albeit with much lower concentrations. We note that the damping of the second shell signal when a Bi pair forms is caused by the broadening of the Bi-As distance distribution and not only by the presence of a Bi-Bi EXAFS path. The Bi-As distances are spread over 0.086 vs 0.022 Å for the random model according to VFF calculations. The first shell Bi-Ga distance spread is smaller: these distances lie within 0.023 Å for the Bi pair vs 0.001 Å in the random case.

In the case of sample C, even if the amplitude of the first shell Fourier peak is almost identical to that of sample A, the second and third shell peak amplitudes and shapes change, suggesting a different organization of the Bi neighbors. A fit with the random model [Fig. 3, top, red (light gray), open squares] fails to reproduce the experimental amplitude of the second and third shell peaks (continuous black line). In case of tetramer formation, the interatomic distances are strongly perturbed by the presence of the Bi next nearest neighbors in the second shell: according to the VFF calculation, the Bi-Ga first shell distances spread over 0.061 Å and the Bi-As second shell ones over 0.10 Å. The fit with the tetramer model [top, olive (light gray), open diamonds] is effective in reproducing the amplitude of the third shell and the region between the second and third shells (where part of the Bi second shell signal is also found). On the contrary it dramatically fails to reproduce the amplitude of the whole second shell peak. By applying the same fitting strategy as for sample B (i.e., weighting the same three modeled local configurations), we obtained a best fit [bottom, blue (dark gray), filled circles] with $37 \pm 19\%$ Bi tetramers and $0 \pm 4\%$ Bi pairs (63% random). This combination models well the experimental Fourier transform, and the agreement is better than that obtained using any other combination involving different short-range order configurations, including other tetramers where Bi atoms are next nearest neighbors of the central one but not next nearest neighbors of each other, triplets with Bi atoms set in a row or in a triangle, or interstitials. Note that the rather long Bi-Bi second shell distance ($R_{Bi\text{-}Bi}$) predicted by VFF in the case of the tetramer of Fig. 3, longer than in any other configuration examined, contributes significantly to the fit quality. Our results indicate that in sample C the number of next-nearest-neighbor Bi atoms around Bi is *on average* close to 1, but that Bi atoms, when they do not remain randomly distributed, tend to aggregate in small clusters rather than in pairs.

Analyzing the average interatomic distances reported in Table II, we remark that there is a trend for the first shell Bi-Ga distance to decrease with increasing Bi concentration: this phenomenon has not been observed in previous experiments on $InAs_{1-x}Bi_x$.[23] We note here that the pseudomorphic deformation of the epilayers has been taken into account in modeling the EXAFS data;[28–30] however, its effect on the interatomic distances is very small (-1.27×10^{-3}, -2.07×10^{-3}, and -2.55×10^{-3} Å for the first shell Bi-Ga distance in samples A, B, and C, respectively). We do not need to arbitrarily increase the Debye-Waller factors or to make them vary in order to account for the different structural disorder in samples with different Bi concentrations: once the correct short-range ordering configuration is found (accounting itself for the nonthermal part of the distances distribution broadening), all spectra are well fitted with the Debye-Waller factors of sample A.

IV. CONCLUSIONS

We have investigated short-range order in $GaAs_{1-x}Bi_x$ alloys as a function of Bi concentration by EXAFS and have found evidence of an evolution from a random distribution of Bi anions to Bi pairing and clustering as the concentration increases. Since the incorporation of the isoelectronic Bi impurity has an effect similar to that of N in lowering the band gap of GaAs,[9,10] and since N clustering in $GaAs_{1-x}N_x$ redshifts the band gap with respect to a random alloy,[17] we think that the deviation from a random distribution of Bi demonstrated in the present work can play an important role in producing the giant optical bowing observed in $GaAs_{1-x}Bi_x$. Moreover, Bi clusters could trap excitons according to a mechanism similar to that proposed for $In_xGa_{1-x}N$,[31] accounting for the PL enhancement observed in these materials despite the low growth temperature and the presence of As antisite defects.

ACKNOWLEDGMENTS

We acknowledge the ESRF for the provision of beamtime through Project No. MA237 and S. Pasternak, R. Steinmann, and F. Perrin for the design of the sample holder. We thank J. L. Fave and C. Barthou (INSP) for discussion.

*Corresponding author; gianluca.ciatto@synchrotron-soleil.fr

[1] J. F. Geisz and D. J. Friedman, Semicond. Sci. Technol. **17**, 769 (2002).
[2] M. Weyers, M. Sato, and H. Ando, Jpn. J. Appl. Phys., Part 2 **31**, L853 (1992).
[3] M. Kondow, K. Uomi, A. Niwa, T. Kitatani, S. Watahiki, and Y. Yazawa, Jpn. J. Appl. Phys., Part 1 **35**, 1273 (1996).
[4] L. H. Li, V. Sallet, G. Patriarche, L. Largeau, S. Bouchoule, L. Travers, and J. C. Harmand, Appl. Phys. Lett. **83**, 1298 (2003).
[5] M. Henini, *Dilute Nitride Semiconductors* (Elsevier, Oxford, UK, 2005).
[6] P. R. C. Kent and A. Zunger, Phys. Rev. B **64**, 115208 (2001).

[7] D. G. Cooke, E. C. Young, F. A. Hegmann, and T. Tiedje, Appl. Phys. Lett. **89**, 122103 (2006).
[8] S. Tixier, M. Adamcyk, T. Tiedje, S. Francoeur, A. Mascarenhas, P. Wei, and F. Schiettekatte, Appl. Phys. Lett. **82**, 2245 (2003).
[9] Y. Zhang, A. Mascarenhas, and L. W. Wang, Phys. Rev. B **71**, 155201 (2005).
[10] S. Francoeur, M. J. Seong, A. Mascarenhas, S. Tixier, M. Adamcyk, and T. Tiedje, Appl. Phys. Lett. **82**, 3874 (2003).
[11] B. Fluegel, S. Francoeur, A. Mascarenhas, S. Tixier, E. C. Young, and T. Tiedje, Phys. Rev. Lett. **97**, 067205 (2006).
[12] A. Janotti, S. H. Wei, and S. B. Zhang, Phys. Rev. B **65**, 115203 (2002).
[13] K. Bertulis, A. Krotkus, G. Aleksejenko, V. Pacebutas, R. Andromavicius, and G. Molis, Appl. Phys. Lett. **88**, 201112 (2006).
[14] K. Kim and A. Zunger, Phys. Rev. Lett. **86**, 2609 (2001).
[15] V. Lordi, V. Gambin, S. Friedrich, T. Funk, T. Takizawa, K. Uno, and J. S. Harris, Phys. Rev. Lett. **90**, 145505 (2003).
[16] G. Ciatto *et al.*, Phys. Rev. B **68**, 161201(R) (2003).
[17] L. Bellaiche and A. Zunger, Phys. Rev. B **57**, 4425 (1998).
[18] A. Filipponi, M. Borowski, D. T. Bowron, S. Ansell, A. D. Cicco, S. D. Panfilis, and J. P. Itié, Rev. Sci. Instrum. **71**, 2422 (2000).
[19] P. A. Lee, P. H. Citrin, P. Eisenberger, and B. M. Kincaid, Rev. Mod. Phys. **53**, 769 (1981).
[20] F. Boscherini, Nucl. Instrum. Methods Phys. Res. B **199**, 169 (2003).
[21] S. Pasternak, F. Perrin, G. Ciatto, H. Palancher, and R. Steinmann, Rev. Sci. Instrum. **78**, 075110 (2007).
[22] B. Ravel and M. Newville, J. Synchrotron Radiat. **12**, 537 (2005).
[23] H. Ofuchi, T. Kubo, M. Tabuchi, Y. Takeda, H. Okamoto, and K. Oe, Jpn. J. Appl. Phys., Suppl. **38**, 545 (1999).
[24] G. Ciatto, J.-C. Harmand, F. Glas, L. Largeau, M. Le Du, F. Boscherini, M. Malvestuto, L. Floreano, P. Glatzel, and R. A. Mori, Phys. Rev. B **75**, 245212 (2007).
[25] A. L. Ankudinov, B. Ravel, J. J. Rehr, and S. D. Conradson, Phys. Rev. B **58**, 7565 (1998).
[26] F. Glas, Phys. Rev. B **51**, 825 (1995).
[27] M. Ferhat and A. Zaoui, Phys. Rev. B **73**, 115107 (2006).
[28] J. C. Woicik, J. G. Pellegrino, B. Steiner, K. E. Miyano, S. G. Bompadre, L. B. Sorensen, T. L. Lee, and S. Khalid, Phys. Rev. Lett. **79**, 5026 (1997).
[29] F. Romanato *et al.*, Phys. Rev. B **57**, 14619 (1998).
[30] M. Tormen, D. De Salvador, M. Natali, A. Drigo, F. Romanato, G. Rossetto, F. Boscherini, and S. Mobilio, J. Appl. Phys. **86**, 2533 (1999).
[31] O. Brandt and K. H. Ploog, Nat. Mater. **5**, 769 (2006).